

DOI: <https://doi.org/10.37434/tpwj2022.08.01>

# DEFORMATION-FREE TIG WELDING OF AMg6 ALLOY WITH APPLICATION OF ELECTRODYNAMIC TREATMENT OF WELD METAL

L.M. Lobanov<sup>1</sup>, V.M. Korzhyk<sup>1</sup>, M.O. Pashchyn<sup>1</sup>, O.L. Mikhodui<sup>1</sup>, A.A. Grynyuk<sup>1</sup>, E.V. Ilyashenko<sup>1</sup>, P.V. Goncharov<sup>1</sup>, P.R. Ustymenko<sup>2</sup>

<sup>1</sup>E.O. Paton Electric Welding Institute of the NASU  
11 Kazymyr Malevych Str., 03150, Kyiv, Ukraine

<sup>2</sup>National Technical University of Ukraine «Igor Sikorsky Kyiv Polytechnic Institute»  
37 Peremohy Prosp., 03056, Kyiv, Ukraine

## ABSTRACT

Application of electrodynamic treatment (EDT), taking into account the welding process peculiarities, is a new trend in engineering practice, enhancing the process capabilities. At the same time, a necessary condition for realization of fusion welding process, is heating of the weld metal with its further cooling to room temperature. Realization of EDT technology during welding promotes more intensive relaxation of welding stresses as a result of EDT, compared to weld metal treatment at room temperature. Proceeding from investigation results, it was found that EDT of butt welded joint samples leads to transition of residual tensile welding stresses into compressive stresses. Experimental verification of the residual stress-strain state with application of the method of electron speckle interferometry confirmed the results of mathematical modeling, namely lowering of tensile stresses and increase of compressive stresses in the weld after EDT at temperature  $T = 150\text{ }^{\circ}\text{C}$ , compared to EDT at  $T = 20\text{ }^{\circ}\text{C}$ . It was proved that EDT of samples of butt joints from AMg6 alloy during TIG welding improves their production accuracy that is characterized by lowering of the level of their residual longitudinal distortion, compared to postweld EDT.

**KEYWORDS:** electrodynamic treatment, electrode device, residual welding stresses, aluminium alloy, electric current pulse, impact interaction, indenter-electrode, membrane stresses, nonconsumable electrode welding

## INTRODUCTION

Residual welding stresses have a negative impact on the fatigue life, corrosion resistance and residual deformations of sheet structures from aluminium-based alloys. In recent years, growth in fabrication of such structures is observed in the world practice so that the problem of reduction of residual tensile stresses becomes particularly urgent. Traditional methods of optimization of the residual stressed states, which involve application of metal-intensive equipment and (or) considerable energy consumption, do not meet the requirements of modern engineering practice [1, 2].

Development of high-technology industries stimulates introduction of energy-saving technologies of deformation-free welding of aluminium-based alloys. Application of pulsed electromagnetic fields (PEMF) for optimization of residual stress-strain states and mechanical characteristics of welded joints is the current trend in modern practice of replacement of the traditional metal processing technologies by advanced and energy-efficient methods [3, 4].

## RESEARCH RELEVANCE

One of the novel approaches to optimization of the residual stressed states of sheet structures is electrodynamic treatment (EDT) of welded joints, which is based on electroplasticity effect (EPE) which arises at

passage of electric current pulses (ECP) of more than  $1\text{ kA/mm}^2$  density through the item metal [5–7]. EPE impact results in appearance of plastic deformations in the metal, initiating the mechanisms of relaxation of residual welding stresses.

In works [8, 9] it was proved that accompanying heating of the zone of electric pulse impact promotes relaxation of tensile stresses. It stimulates investigations of new EDT capabilities, one of which is its application during fusion welding.

It should be noted that no assessment of the influence of thermal cycle of welding on the features of residual stressed state regulation under EDT impact has not been performed up to now.

In view of the above-said, the objective of the work is development of scientific fundamentals of welding technology with EDT application for regulation of the residual stress-strain states of aluminium alloy welded joints.

Considering the data of work [9], it can be noted that EDT under the conditions of weld metal heating is more effective (compared to EDT without heating) for lowering of residual stresses in aluminium alloy welded plates. Here, as noted above, the source of such heating can be the heat of the cooling welded joint.

Hardware support of the method is reduced to organizing synchronous movement of the welding torch

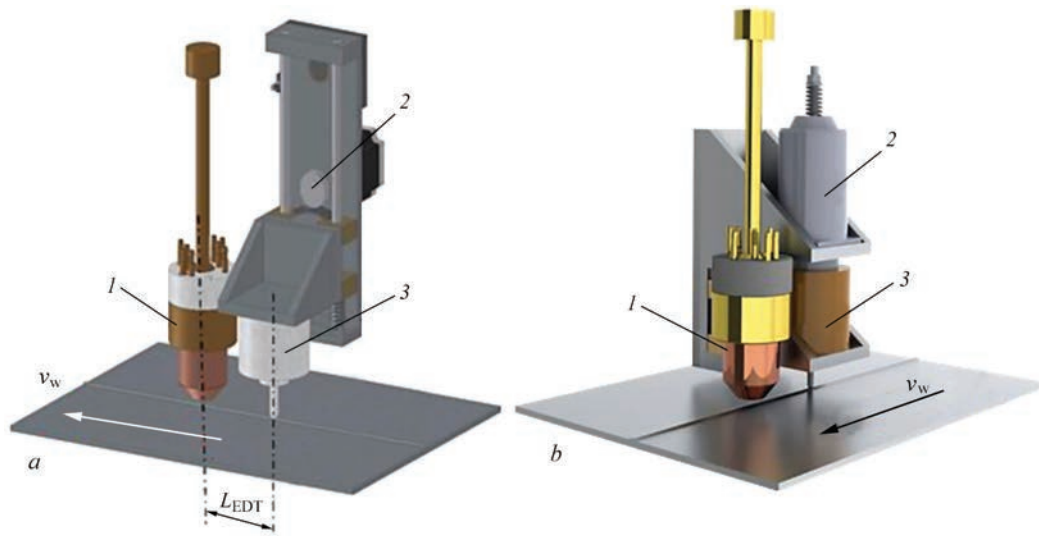


**Figure 1.** Variants of design schemes of EDT during welding with monoblock layout of the end effectors: *a* — EDT ED pressing to the weld metal with application of eccentric 2; *b* — EDT ED pressing to the weld metal with application of linear displacement solenoid 2 ( $v_w$  — welding direction; 1 — WT; 3 — EDT ED)

(WT) and electrode device for EDT (EDT ED) that are designed as a monoblock with a device recording their relative position. Figure 1 shows the design variants of portal type schemes of EDT ED and WT with monoblock layout. Design variants of electrode movement ensure reliable electric contact of the electrode with weld metal at the moment of electrodynamic impact. Contact interaction of EDT ED with the weld metal can be performed on the base of a mechanical drive, using an eccentric (Figure 1, *a*) or electric drive, using linear displacement solenoid (Figure 1, *b*). Each of the schemes in Figure 1 has its advantages and disadvantages, discussion of which goes beyond the scope of this work.

Application of these schemes allows ensuring optimum distance  $L_{EDT}$  between EDT ED and WT. The monoblock includes EDT ED — 3 and WT — 1,



**Figure 2.** Hardware complex for automatic TIG welding which is compatible with weld EDT: 1 — system for filler wire feeding; 2 — welding torch; 3 — electrode device; 4 — linear displacement solenoid of EDT electrode

which are installed along the welded joint at distance  $L_{EDT}$  between 1 and 3 (Figure 1, *a*). Value  $L_{EDT}$  sets the heating temperature  $T_{EDT}$  of treatment zone under the conditions of impact of thermal cycle of welding. Power networks for welding and EDT are formed independently one from the other.

Searching for optimal EDT mode under the welding conditions involves experimental evaluation of the electrophysical and mechanical characteristics of the treated material. An alternative solution of the problem is mathematical modeling of EDT process, which allows assessment of the evolution of stress-strain states of the welded joints as a result of EDT. In keeping with modeling results, optimal  $T_{EDT}$  value at EDT of AMg6 alloy is 150 °C [10–13].

## PROCEDURE AND RESULTS OF EXPERIMENTAL STUDIES OF THE INFLUENCE OF WELDING THERMAL CYCLE ON THE RESIDUAL STRESS-STRAIN STATES

A hardware complex for automatic TIG welding of aluminium alloys, which is compatible with EDT process, was made for implementation of the technology of EDT during welding (Figure 2). The complex components are designed as a monoblock.

In order to assess the effectiveness of EDT during welding, the method of electron speckle-interferometry was used [14] to conduct comparative studies of residual stress-strain states of welded joints from AMg61 alloy made with EDT application after and during welding, i.e. at  $T$  values of 20 and 150 °C, respectively. Experimental evaluation of the longitudinal (along the weld line) component  $\sigma_x$  (Figure 3, *a*) of residual welding stresses and deflections  $f_x$  of lon-

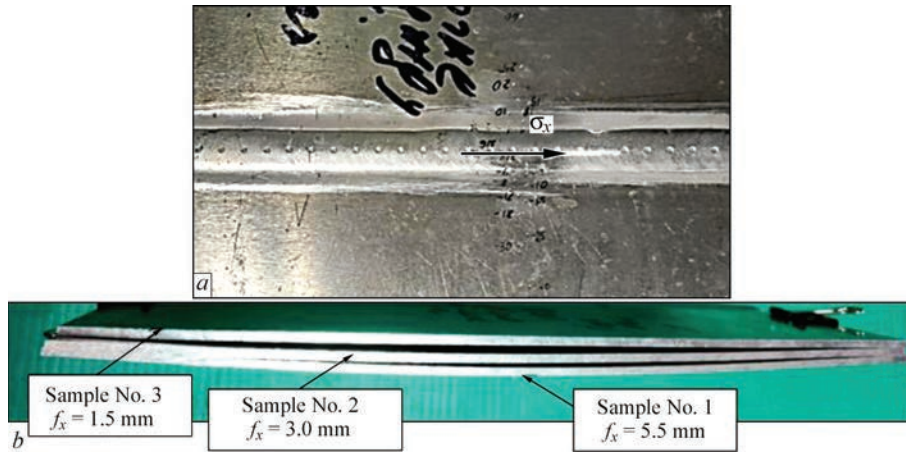


**Figure 3.** Appearance of samples Nos 1–3: *a* — sample No.2; where EDT point zones are located on the weld; arrow shows the direction of action of stress component  $\sigma_x$ ; *b* — longitudinal deflections  $f_x$  of the edge of samples Nos 1–3

**Table 1.** Mode of TIG welding of welded joint sample from AMg61

Arc voltage $U_{arc}$ , V	Arc current $I_{arc}$ , A	Welding speed $v_w$ , mm/s	Wire feed rate $v_f$ , mm/s	Argon flow rate $v_{Ar}$ , l/min	Filler wire diameter $d$ , mm
16.2	160	3.3	23.3	15	1.2

gitudinal edges of the samples was performed using calipers and planed ruler [5].

Samples of butt welded joints from AMg61 alloy plates of  $450 \times 200 \times 3$  mm size were prepared, in order to study the thermal impact of EDT (Figure 3). Samples were welded from two plates of  $450 \times 100 \times 3$  mm size by TIG process in argon in the mode given in Table 1, under the conditions of resting on a rigid foundation. Wire of ER5356 grade was used as filler material.

Sample No. 1 was produced without EDT application. Sample No. 2 (Figure 3, *a*) was welded without treatment and was subjected to EDT after welding at  $T = 20$  °C. On sample No. 3 EDT was performed during welding at  $T = 150$  °C. EDT of samples 2 and 3 was performed at similar values of treatment mode parameters that ensures the energy of single electrodynamic action at the level of 1 kJ.

Depth  $h$  of point zone (pits) of EDT impact and weld reinforcement height were equal to 0.2 and 0.6 mm, respectively. Thus, depth  $h$  of the pits was not higher than weld reinforcement height, i.e. it did not reduce the area of welded joint working section. It causes a negative impact of the pits on the mechanical characteristics of welded joints [5, 6]. Distance between the point zones of EDT action was 5.0 mm (Figure 3, *a*).

Figure 3, *b* shows the comparison of residual deflections  $f_x$  of longitudinal edges of samples Nos 1–3. One can see that EDT after and during welding reduces  $f_x$  value 1.8 and 3.7 times, respectively. This fact can be explained both by relaxation of residual stresses as a result of EDT, and by “rigid” fixation of

the plates. It eliminated their vertical displacement during welding and promoted formation of residual tensile plastic deformations in the weld. Interaction of the latter with residual compressive deformations from welding resulted in reduction of deflections  $f_x$ .

Figures 4–6 give the distributions of residual stresses  $\sigma_x$  in samples Nos 1–3, which are characterized by some common features. So, in the initial state,  $\sigma_x$  values in the weld center are smaller than on the outer side of the plate (curve 1 — top), compared with the sample reverse side (curve 3 — bottom). This is attributable to more intensive heat removal from the open outer surface of the sample, compared to the reverse surface, which contacts the absolutely rigid base — the welding table, which is the heat shield. Half-width of the zone of peak values of residual tensile  $\sigma_x$  in samples Nos 1–3 did not exceed 15 mm. Considering the fact that EDT was performed along the weld center in all the experiments, further com-

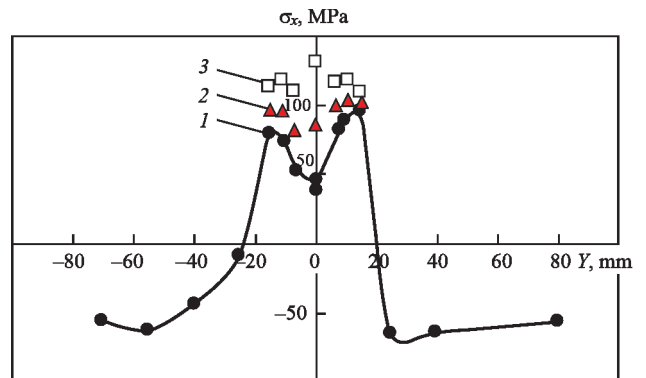


**Figure 4.** Distribution of stresses  $\sigma_x$  in the central cross-section of sample No. 1: curve 1 — top; 2 — membrane stresses; 3 — bottom

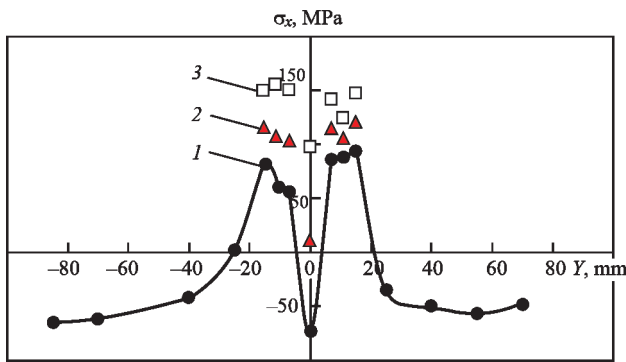


**Figure 5.** Distribution of stresses  $\sigma_x$  in the central cross-section of sample No. 2: curve 1 — top; 2 — membrane stresses; 3 — bottom

parative evaluation of the stressed states of the treated zone was performed in the samples.

In the initial state tensile  $\sigma_x$  values in the weld center in sample No.1 reached 50 and 130 MPa, respectively, on the outer (curve 1 — top) and reverse (curve 3 — bottom) sides of the plate (Figure 4). Evaluation of membrane stresses  $\langle \sigma_x \rangle$  was performed without allowing for the out-of-plane bending component (curve 2). Values  $\langle \sigma_x \rangle$  were calculated as an average between experimentally determined  $\sigma_x$  on curves 1 and 2. Values  $\langle \sigma_x \rangle$  in the weld center were not higher than 90 MPa.

After EDT at  $T = 20^\circ\text{C}$ ,  $\sigma_x$  values in the center of the weld of sample No. 2 reached  $-75$  and  $100$  MPa, respectively on the outer (curve 1 — top) and reverse (curve 3 — bottom) sides of the plate (Figure 5). Thus, after EDT tensile stresses  $\sigma_x$  in the contact zone were transformed into compressive stresses, but on the plate reverse side tensile stresses  $\sigma_x$  decreased by 20 %. Tensile membrane stresses  $\langle \sigma_x \rangle$  in the weld center did not exceed 12 MPa, i.e. they decreased to 90 %. Analyzing the data in Figure 5, one can see that EDT at  $T = 20^\circ\text{C}$  has a dominant influence on the stressed state of the plate contact surface and a much weaker one — on  $\sigma_x$  values on the reverse side of sample No. 2.

After EDT at  $T = 150^\circ\text{C}$ ,  $\sigma_x$  values in the center of the weld of sample No. 2 reached  $-100$  and  $10$  MPa, respectively on the outer (curve 1 — top) and reverse (curve 3 — bottom) sides of the plate. Thus, after EDT tensile  $\sigma_x$  stresses in the contact zone transformed into compressive stresses, and on the reverse side tensile  $\sigma_x$  decreased by more than 90 %. Compressive membrane

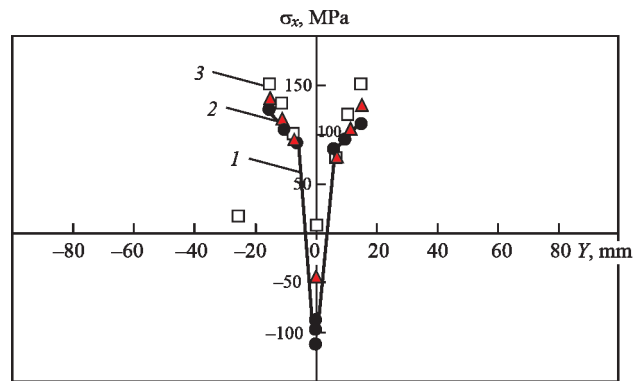


**Figure 6.** Distribution of stresses  $\sigma_x$  in the central cross-section of sample No. 3: curve 1 — top; 2 — membrane stresses; 3 — bottom

stresses  $\langle \sigma_x \rangle$  in the weld center reached  $-50$  MPa, i.e. after EDT they changed their sign. Analyzing the data in Figure 6, one can see that EDT at  $T = 150^\circ\text{C}$  makes a significant influence on the stressed state of the contact and reverse surfaces of sample No. 3.

Results of modeling [10] and experimental studies of residual stresses  $\sigma_x$  in samples Nos 1–3 are generalized in the comparative Table 2. It should be noted that in terms of quality the experimental data confirm the results of mathematical modeling of the residual states of plates from AMg61 alloy after EDT at temperatures  $T = 20$  and  $150^\circ\text{C}$ .

Experimental results of assessment of stresses  $\sigma_x$  in sample No.1 (row 1) with those of samples No. 2 (row 2) and No. 3 (row 4) were compared. Note that EDT promotes transition of tensile stresses into compressive stresses in the contact zone, and thermal impact promotes increase of  $\sigma_x$  values.

EDT at  $T = 20^\circ\text{C}$  promotes transformation of tensile stresses  $\sigma_x$  in the contact zone into compressive stresses (column 3), which is visible at comparison of rows 1 and 2. Thermal influence intensifies the relaxation mechanisms, activated by EDT that promotes formation of greater values of compressive stresses  $\sigma_x$  (comparison of rows 2 and 4).

EDT at  $T = 20^\circ\text{C}$  promotes lowering of tensile stresses of AMg61 near the rigid base (column 4) which can be seen from comparison of rows 1 and 2. Thermal impact intensifies the relaxation mechanisms activated by EDT (comparison of rows 2 and 4).

**Table 2.** Results of experimental studies of residual welding stresses  $\sigma_x$  in samples Nos 1–3

Number	Sample characteristic		$\sigma_x$ , MPa, top	$\sigma_x$ , MPa, bottom	$\langle \sigma_x \rangle$ , MPa
1	2		3	4	5
1	Sample No. 1 without EDT	Experiment (Figure 4)	50	130	90
2	Sample No. 2	Experiment (Figure 5)	$-75$	100	12
3	EDT at $T = 20^\circ\text{C}$	Modeling	$-132$	$-109$	$-156$
4	Sample No. 3	Experiment (Figure 6)	$-100$	10	$-45$
5	EDT at $T = 150^\circ\text{C}$	Modeling	$-142$	$-127$	$-155$

At the respective comparison of rows 2 and 3 and 4 and 5 one can see that modeling yields greater values of stresses after EDT than does the experiment. This is attributable to ignoring (at modeling) the convective heat removal from the sample surfaces which may lower the characteristics of accompanying heating of the plates that promotes reduction (relative to calculated values) of EDT effectiveness. In the contact zone (column 3) calculated  $\sigma_x$  are 1.4–1.7 times higher than the experimental values. It is true for both the calculated and experimental compressive  $\sigma_x$  values. While at modeling the thermal impact increases the compressive  $\sigma_x$  values up to 8 % (comparison of rows 3 and 5), in the experiment it is up to 30 % (rows 2 and 4) at smaller absolute values of the latter.

The nature of  $\sigma_x$  distribution near the plate resting on the rigid base (column 4) is different. While in the experiments  $\sigma_x$  stresses after EDT are tensile (rows 2 and 4), in the calculation they are compressive (rows 3 and 5). Therefore, based on comparison of the experimental data, the effectiveness of EDT as a method of controlling  $\sigma_x$  on the reverse side is lower — bottom, compared to the outer side — top. However, the influence of the thermal impact on the Bottom side increases essentially, which leads to lowering of tensile  $\sigma_x$  values by 70 % after EDT at  $T = 150$  °C, compared to  $T = 20$  °C (comparison of rows 4 and 2, respectively).

Thus, essential lowering of  $\langle \sigma_x \rangle$  (column 5) under the impact of heating is determined by relaxation of stresses near the rigid base — bottom (comparison of rows 2 and 4). At modeling  $\sigma_x$  lowering is only up to 16 % (comparison of rows 3 and 5), which is explained by ignoring the convective heat removal which was proved above.

Considering the results in Figures 4–6 and Table 2 one can conclude that the thermal impact, accompanying EDT, is an effective regulator of the influence on stressed-strained states of welded joints from aluminium-based alloys with the purpose of their optimization.

Residual compressive stresses decelerate propagation of fatigue fracture of welded joint metal [5, 6]. Proceeding from the above data, EDT during welding should be regarded as a promising method to optimize the stress-strain states and increase the accuracy of sheet welded structures from aluminium alloys. This technology can be used under industrial conditions for deformation-free welding of thin-walled shell and panel structures in aerospace engineering, where stringent requirements are traditionally made of their aerodynamic characteristics and stressed states. EDT application during welding will promote shortening of the time of item manufacturing and extension of their life.

## CONCLUSIONS

1. It was proved that application of electrodynamic treatment (EDT) of weld metal which is performed as one process in synchronism with arc welding, is more effective, compared to separate EDT after welding, which is expressed in a more optimal residual stress-strain state of the finished welded joint.

2. Experimental check of the residual stress-strain state with application of the method of electron speckle-interferometry confirmed the results of mathematical modeling, namely lowering of the tensile stresses and increase of compressive stresses in the weld after EDT at temperature  $T = 150$  °C, compared to EDT at  $T = 20$  °C.

3. It was proved that EDT of butt joint samples from AMg61 alloy during welding improves their manufacturing accuracy which is characterized by lowering of the level of their residual longitudinal distortion, compared to EDT after welding.

4. It was found that EDT of butt joint samples from AMg6 (1561) alloy during nonconsumable electrode arc welding promotes optimization of their stressed states, which is characterized by lowering of residual tensile welding stresses in the weld up to 70 %, compared to EDT after welding.

## REFERENCES

1. Madi, Y., Besson, J. (2014) *Effect of residual stresses on brittle fracture*. Mat. ECRS-9. UTT, Troyes, France.
2. Masubuchi, K. (1980) *Analysis of welded structures*. Pergamon Press, Oxford, United Kingdom.
3. Shao, Quan, Kang, Jiajie, Xing, Zhiguo et al. (2019) Effect of pulsed magnetic field treatment on the residual stress of 20Cr<sub>2</sub>Ni<sub>4</sub>A steel. *J. of Magnetism and Magnetic Materials*, **476**, 218–224.
4. Stepanov, G.V., Babutskii, A.I., Mameev, I.A., et al. (2011) Redistribution of residual welding stresses in pulsed electro-magnetic treatment. *Strength of Materials*, **43**(3), 326–331. DOI: <https://doi.org/10.1007/s11223-011-9300-2>
5. Lobanov, L.M., Pashchyn, N.A., Kondratenko, I.P. et al. (2018) Development of post-weld electrodynamic treatment using electric current pulses for control of stress-strain states and improvement of life of welded structures. *Mater. Performance and Characterization*, **7**, 4. DOI: <https://doi.org/10.1520/MPC20170092>
6. Lobanov, L.M., Pashchyn, M.O., Tymoshenko, O.M. et al. (2020) Increase in the life of welded joints of AMg6 aluminium alloy. *The Paton Welding J.*, **4**, 2–8. DOI: <https://doi.org/10.37434/as2020.04.01>
7. Conrad, H., Sprecher, A. (1989) *The electroplastic effect in metals*. Elsevier Sci. Publishers B.V., Dislocations in Solids Ed. by F.R.N. Nabarro.
8. Stepanov, G.V., Babutskii, A.I., Mameev, I.A. (2004) High-density pulse current-induced unsteady stress-strain state in a long rod. *Strength of Materials*, **36**, 377–381. DOI: <https://doi.org/10.1023/B:STOM.0000041538.10830.34>
9. Lobanov, L.M., Pashchyn, M.O., Mikhodui, O.L. et al. (2022) Electrodynamic treatment of welded joints of aluminium AMg6 alloy in the process of heating the weld metal. *The Paton Welding J.*, **4**, 3–7. DOI: <https://doi.org/10.37434/as2022.04.01>

10. Lobanov, L.M., Pashchyn, M.O., Mikhodui, O.L., Sydorenko, Yu.M. (2017) Effect of the indenting electrode impact on the stress-strain state of an AMg6 alloy on electrodynamic treatment. *Strength of Materials*, 49(3), 369–380. DOI: <https://doi.org/10.1007/s11223-017-9877-1>
11. Sydorenko, Y.M., Pashchyn, M.O., Mikhodui, O.L. et al. (2020) Effect of pulse current on residual stresses in AMg6 aluminum alloy in electrodynamic treatment. *Strength of Materials*, 52(5), 731–737. DOI: <https://10.1007/s11223-020-00226-2>
12. Lobanov, L.M., Pashchyn, M.O., Mikhodui, O.L., Sydorenko Yu.M. (2018) Electric pulse component effect on the stress state of AMg6 aluminum alloy welded joints under electrodynamic treatment. *Strength of Materials*, 50(2), 246–253. DOI: <https://10.1007/s11223-017-9862-8>
13. Lobanov, L.M., Pashchyn, M.O., Mikhodui, O.L., Sydorenko Yu.M. (2022) Calculated evaluation of stress-strain states of welded joints of aluminium AMg61 alloy under the action of electrodynamic treatment of weld metal in the process of fusion welding. *The Paton Welding J.*, 7, 3–8. DOI: <https://doi.org/10.37434/as2022.07.01>
14. Lobanov, L.M., Pashchyn, M.O., Mikhoduj, O.L., Khokhlova, J.A. (2016) Investigation of residual stresses in welded joints of heat-resistant magnesium alloy ML10 after electrodynamic treatment. *J. of Magnesium and Alloys*, 4(2), 77–82. DOI: <https://10.1016/j.jma.2016.04.005>

#### ORCID

L.M. Lobanov: 0000-0001-9296-2335,  
V.M. Korzhyk: 0000-0001-9106-8593,  
M.O. Pashchyn: 0000-0002-2201-5137,  
O.L. Mikhodui: 0000-0001-6660-7540,  
E.V. Ilyashenko: 0000-0001-9876-0320

#### CONFLICT OF INTEREST

The Authors declare no conflict of interest

#### CORRESPONDING AUTHOR

M.O. Pashchyn  
E.O. Paton Electric Welding Institute of the NASU  
11 Kazymyr Malevych Str., 03150, Kyiv, Ukraine.  
E-mail: [svarka2000@ukr.net](mailto:svarka2000@ukr.net)

#### SUGGESTED CITATION

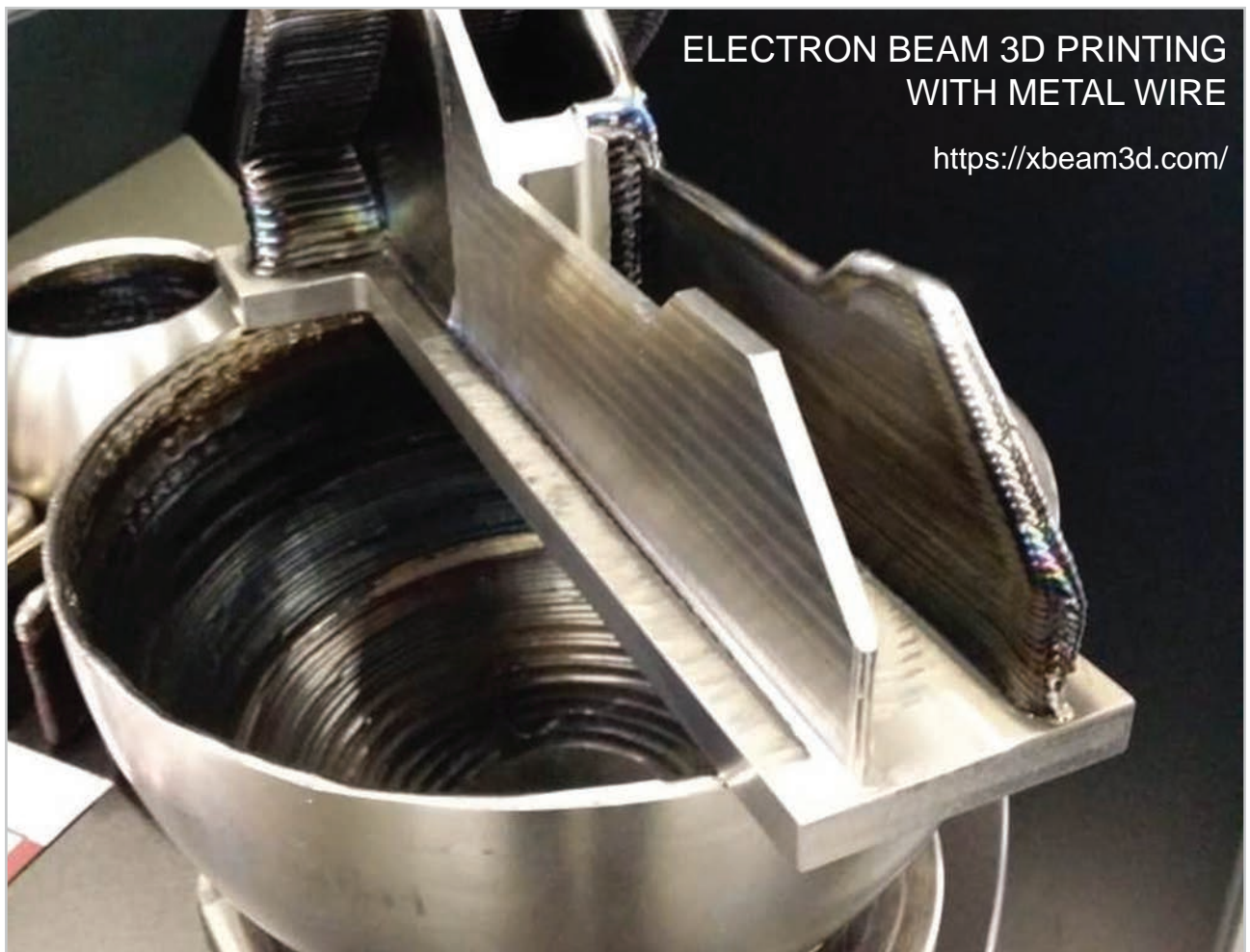
L.M. Lobanov, V.M. Korzhyk, M.O. Pashchyn,  
O.L. Mikhodui, A.A. Grynyuk, E.V. Ilyashenko,  
P.V. Goncharov, P.R. Ustymenko (2022)  
Deformation-free TIG welding of AMg6 alloy with  
application of electrodynamic treatment of weld  
metal. *The Paton Welding J.*, 8, 3–8.

#### JOURNAL HOME PAGE

<https://pwj.com.ua/en>

Received: 21.06.2022

Accepted: 17.10.2022



**ELECTRON BEAM 3D PRINTING  
WITH METAL WIRE**

<https://xbeam3d.com/>